ELSEVIER

Journal of Nuclear Materials 244 (1997) 195–204

journal of nuclear materials

Non-steady-state conditions and incascade clustering in radiation damage modeling [1]

R.E. Stoller *

Metals and Ceramics Division, Oak Ridge national Laboratory, P.O. Box 2008, Oak Ridge, TN 37831-6376, USA

Received 4 September 1996; accepted 15 November 1996

Abstract

The results of molecular dynamics simulations of displacement cascades indicate that a large fraction of the point defects that survive after intracascade annealing may be found in clusters, rather than as individual point defects. In addition, the mobility of these small point defect clusters may be relatively high. The impact of these clusters is discussed in the framework of a radiation damage model for austenitic stainless steel using the chemical reaction rate theory. Although this theory has been broadly applied in models simulating such radiation-induced phenomena as void swelling, irradiation creep, and embrittlement, such models have generally not fully accounted for incascade clustering. Many of these models have also focused on the assumed steady state behavior and tended to neglect the explicit dose and temperature dependence of the sink structure. A previously-developed model has been modified to permit a more extensive investigation of the time (dose) dependence of the point defect and extended defect concentrations and of the impact of incascade clustering. A preliminary evaluation of the so-called production bias was also carried out with this model. The results indicate that defect behavior is complex and that the limiting behavior predicted by simple analytical solutions is frequently not achieved. The comparison of the production bias and the conventional dislocation/interstitial bias found that two were comparable if examined separately at 500°C, but that the production bias effect was minimized in the presence of a reasonable dislocation/interstitial bias.

1. Introduction

The chemical reaction rate theory has been extensively used in radiation damage models that simulate and predict phenomena such as void swelling, irradiation creep and radiation-induced hardening or embrittlement [1–6]. Although the agreement between the predictions of such models and experimental data is generally good, their use has been somewhat limited by uncertainties in the choice of parameters such as point defect formation and migration energies, interfacial energies, and even primary defect formation parameters. Further, different values for the extended defect sink strengths must be used depending on whether point defect absorption is controlled by point defect diffusion to the sinks or point defect absorption at the sink surface [2]. An additional limitation of many models is the assumption of steady state point defect concentrations. Such models can not be applied to steels for irradiation temperatures much lower than about 250 to 300°C [5,7,8]. This temperature range is of interest for some out-of-core components in current fission reactors, as well as for near-term fusion reactors. Moreover, the conventional rate theory can give results which are not physically realistic if applied for temperatures below about 50°C; calculated sink strengths and point defect concentrations can be too high unless special precautions are taken.

The issue of primary defect formation has received considerable attention in recent years. Advances in computing capability have permitted the method of molecular dynamics (MD) to be applied to the problem of simulating atomic displacement cascades in a much more extensive

* Fax: +1-423 574 0641; e-mail: stollerre@ornl.gov.

[1] Research sponsored by the Division of Materials Sciences, U.S. Department of Energy under contract DE-AC-5-84OR21400 with Lockheed Martin Energy Systems, Inc.

PII S0022-3115(96)00737-4

way [9–16]. Published results for MD simulation energies up to 25 keV have provided new information on both the number of point defects that survive intracascade annealing and the distribution of these defects. Cascade simulations have been carried out in a broad range of materials and the qualitative aspects of primary defect production are similar in each case. In addition, as discussed in Refs. [12,15], the MD predictions appear to be consistent with the limited experimental observations to which they can be directly compared. Although impurities and alloying elements are likely to alter some of the details observed, this generality at least partially justifies the application of the MD results from pure metals in radiation damage models developed for engineering alloys.

A typical example of the MD results is provided by ten 20 keV MD cascade simulations of iron at 100 K. In this case, the average number of point defects that escaped intracascade annealing was 60 [13,14] or 0.3 times the number of defects that would be calculated using the standard NRT model [17]. Only about 40% of the interstitials were in the form of isolated monodefects; 60% were contained in clusters that had formed directly within the cascade. These clusters contained from 2 to 13 interstitials. Although extensive vacancy clustering has been observed in similar MD simulations of copper cascades [9,10,12], little incascade vacancy clustering has been reported to date in iron [11–14] for the simulation times accessible by MD. However, a recent reanalysis of high-energy iron cascades has found strong evidence of incipient vacancy clusters that could easily be formed within a few atomic jumps [18].

A particularly interesting observation was that the interstitial clusters were quite mobile. The apparent activation energy for cluster migration was no more than a few tenths of an eV [13,19]. This cluster mobility is particularly significant in light of what has been termed the 'production bias' mechanism for driving microstructural evolution [20–22]. This mechanism relies on an effective bias which is produced when a greater fraction of the radiation-produced vacancies than interstitials are in the form of mobile monodefects. However, unless the interstitial clusters can be removed efficiently from the system, an unrealistically high concentration of the clusters would accumulate. A high cluster mobility would permit the clusters to glide or diffuse to sinks.

In the work discussed here, the impact of the MD results is explored using a previously developed model of microstructural evolution [4]; a brief summary of the model will be given below. After reviewing the basic behavior of the model and demonstrating its agreement with a range of data, the impact of several modifications will be described. These include: relaxation of the assumption of steady-state point defect concentrations in order to explore a broader range of irradiation temperatures, the impact of incascade interstitial clustering on the dose and temperature dependence of the model's predictions, and a preliminary evaluation of the 'production bias' vis a vis the conventional dislocation bias as a mechanism for driving microstructural evolution.

2. Description of model employed

2.1. Initial model development

The basic model employed in this work was developed to investigate the effects of fast neutron irradiation on microstructural evolution in austenitic stainless steels; it is described in Ref. [4]. Briefly, this composite model simulated the evolution of the dislocation structure, cavities (helium-stabilized bubbles and voids), and transient vacancy clusters formed by cascade collapse. These vacancy clusters are thermally unstable but can still reach an appreciable density at high dose rates. The dislocation component of the model included both thermal and radiation-induced mechanisms for dislocation formation and dislocation recovery. The formation and growth of Frank faulted interstitial loops provided the primary source term for the dislocation network. The conventional dislocation/interstitial bias was applied to both the dislocation network and the faulted dislocation loops with a higher bias for the loops than for line dislocations. The subgrain structure observed in cold-worked materials was included as a static sink. Simulations of 20% cold worked material were initiated with a network dislocation density of 3×10^{15} m^{-2} and an initial value of 3×10^{12} m^{-2} was used for solution annealed material.

The time dependence of the extended defects, including incascade vacancy clusters was explicitly included in the rate equations describing their evolution. Typically, a point defect cascade survival efficiency of (i.e. the fraction of the NRT displacements) 25 to 33% was used and up to 60% of the surviving vacancies were assumed to be found in the transient incascade clusters. The point defect concentrations and the concentrations of di-, tri-, and tetra-interstitial clusters were calculated assuming quasi-steady-state. Since incascade interstitial clustering was not included in the model, these small interstitial clusters were able to form only by essentially classical nucleation. The tetra-interstitial was assumed to be the stable nucleus for Frank loop formation.

Using a set of reasonable material parameters for austenitic stainless steel [4,23], the predictions of this model were shown to be in good agreement with a broad range of experimental data. This is illustrated in Figs. 1–3, where the predicted swelling, network dislocation density, and faulted loop density, respectively, are compared with relevant data [4,24–31]. The ability to obtain such agreement for temperatures from 350 to 700°C and doses up to 100 dpa indicates the potency of this basic rate theory approach and the dislocation/interstitial bias as a mechanism for promoting the point defect partitioning required

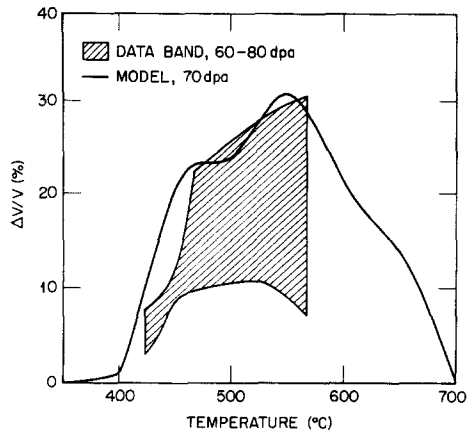

Fig. 1. Comparison of predicted swelling at 70 dpa and fast reactor swelling data at 60 to 80 dpa [4,24].

to obtain net microstructural evolution. The most obvious discrepancy between the predictions and the data in Fig. 3 is the dislocation loop density at the lower temperatures; as will be shown below, this is partially due to the assumption of steady state point defect concentrations.

One important aspect of the computer code used to implement this model was a detailed accounting of the fate of all the point defects produced; this is essentially equivalent to verifying conservation of mass as the simulation proceeds. An example of this accounting is shown in Figs. 4 and 5 which demonstrate the relative importance of the principle vacancy sinks by plotting the fraction of the total

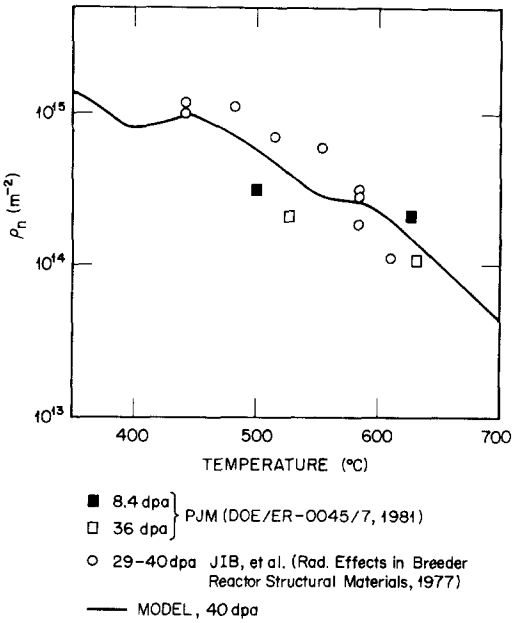

Fig. 2. Comparison of predicted network dislocation density and fast reactor data at 40 dpa [4,25,26].

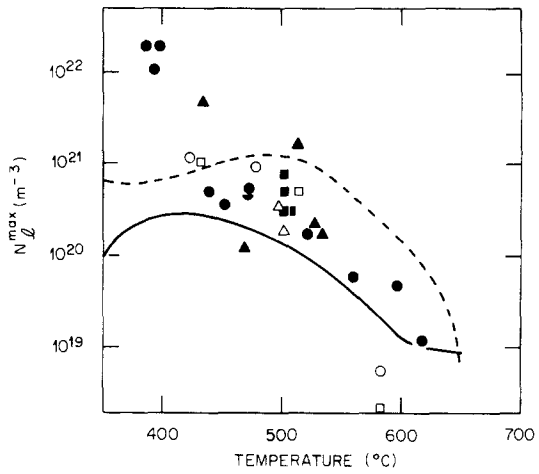

MODEL, $\rho_n(0) = 3 \times 10^{15}$ m^{-2}
MODEL, $\rho_n(0) = 3 \times 10^{13}$ m^{-2}
● HRB AND JLS (JNM 46), SA 316
▲ PJB, BEL AND DAS (JNM 67), SA 316
○ HRB (JNM 57), CW 316
△ HRB, FAG AND GLG (JNM 66), CW 316
■ HRB, FAG AND GLG (JNM 66), SA 316
□ EEB AND JOS (ASTM STP 529), SA 316

Fig. 3. Comparison of predicted maximum faulted loop density and low-fluence fast reactor data [4,27–31].

vacancies absorbed by each sink. The temperature dependence of the fractional vacancy absorption at 100 dpa is shown in Fig. 4 and the fluence dependence of this same parameter is shown in Fig. 5 for a temperature of 450°C. Notable in Fig. 4 is the fact that bulk or matrix recombination of point defects does not reach an appreciable level until low sink strengths are obtained at relatively high irradiation temperatures. Although the results shown in Figs. 4 and 5 are for 20% cold worked material, similar values are observed for solution annealed material. Addi-

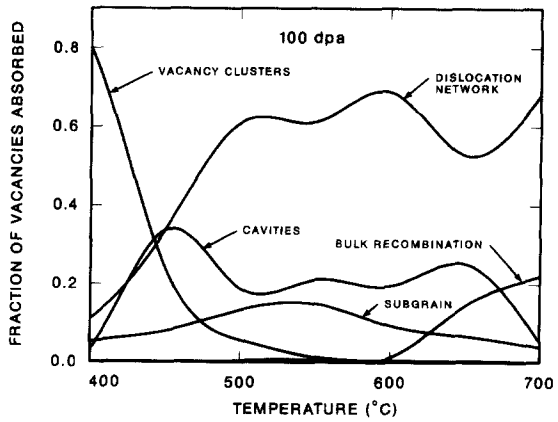

Fig. 4. Fraction of total vacancies lost to various sinks at 100 dpa, 20% cold-worked material.

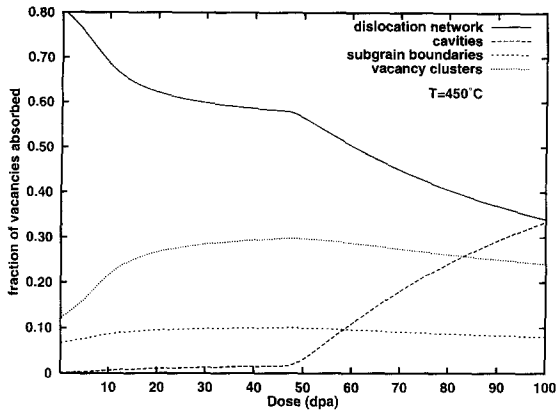

Fig. 5. Fraction of total vacancies lost to various sinks at 450°C, 20% cold-worked material.

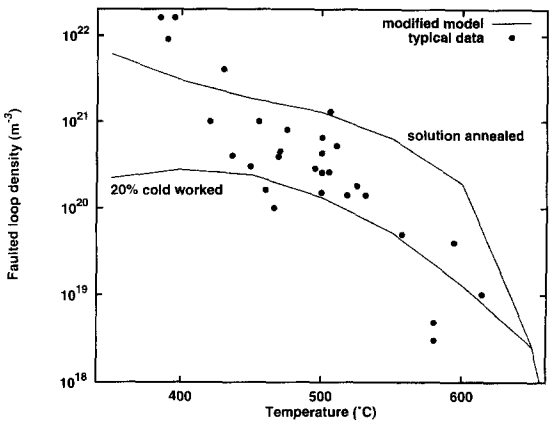

Fig. 6. Comparison of low-fluence fast reactor data [27–31] and predicted maximum faulted loop density with time dependent point defect concentrations.

tional details on the development and predictions of this model can be found in Ref. [23].

2.2. Modifications to model: Relaxation of the steady state assumption

The first modification to the model was recasting the rate equations to eliminate the assumption of steady state point defect concentrations. This simply involved the explicit integration of the rate equations describing the population of vacancies, interstitials, and di-, tri-, and tetra-interstitial (Eqs. (2–6) from Ref. [4]) along with the rate equations describing the extended defects. As expected, this had essentially no impact on the predictions of the model for temperatures greater than about 400°C. Even at 350°C, the changes in the calculated void swelling and network dislocation density were not significant. The swelling was reduced from 0.08% to 0.06% and the dislocation density increased from 4.3×10^{14} to 4.8×10^{14} m^{-2}.

The impact of the steady state point defect assumption on the faulted dislocation loop density was somewhat greater. Compared to the values obtained with the assumption of steady state point defect concentrations, the maximum loop density at 350°C increased by 2.5 times for 20% cold worked material and by a factor of 28 for solution annealed material. The maximum loop density predicted by the modified model is shown in Fig. 6 along with the same data that was plotted in Fig. 3. A comparison of Figs. 3 and 6 demonstrates that the revised model gives improved agreement with the microstructural observations. The increased loop density is the result of a higher nucleation rate since the actual interstitial concentration exceeds the steady state value for the first 10 dpa.

In order to further explore the transition region from near-steady-state to transient behavior, additional calculations were carried out at somewhat lower temperatures. The results provide further evidence of the need to critically evaluate the applicability of the steady state assumption for low to intermediate irradiation temperatures. For example, the calculated vacancy and interstitial concentrations are shown in Fig. 7a and b for temperatures of 325

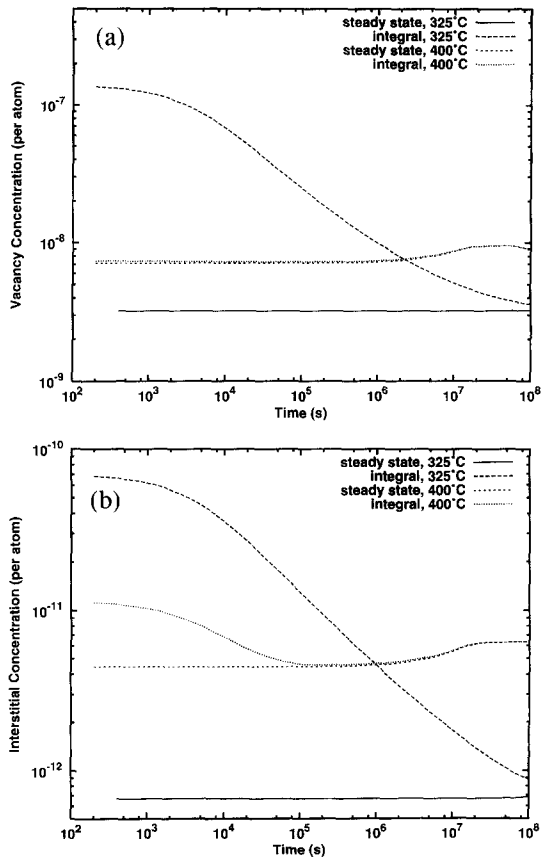

Fig. 7. Calculated vacancy (a) and interstitial (b) concentrations from the steady state and time-dependent model at 325 and 400°C.

and 400°C. Results of steady state and time-dependent calculations are compared and the time required to approach steady state behavior can be seen to increase from ~ 1 day at 400°C to ~ 3 years at 325°C.

The behavior of the point defect concentrations shown in Fig. 7 is in one respect different from earlier discussions of the point defect transient [5,7,8]. For example, the lengthy point defect transient at temperatures below about 200°C was invoked as an explanation for the much higher than expected irradiation creep observed in stainless steel at 60°C [5]. In this case, the point defect transient was controlled by the time required for vacancies to diffuse to sinks and the interstitial concentration was greater than its steady state value for a considerable period. This led to excessive dislocation climb, and creep, as the dislocations absorbed the excess interstitials.

This can not be the explanation for the behavior shown in Fig. 7 since the time for the vacancy concentration to reach steady state should be only on the order of 10 to 100 s at 325 to 350°C [5]. In addition, both the vacancy and interstitial concentrations are shown to be decreasing during the transient illustrated in Fig. 7 while for the case discussed in Ref. [5] the vacancy concentration was increasing toward steady state while the interstitial concentration was decreasing. In the case illustrated by Fig. 7, the evolution of the point defect concentrations is controlled by microstructural transients. The strong initial transient is due to the evolution of the unstable, incascade vacancy clusters and their approach to a near steady state condition. The recovery of the network dislocation density and the build up of the dislocation loop population also contribute to this transient. An additional, weaker transient can be seen at times longer than 10^7 s at 400°C as the cavity sink strength due to voids begins to be significant.

Essentially the same microstructural transients give rise to the dose dependence of the fractional vacancy absorption plotted in Fig. 5. Taken together with the temperature dependence shown in Fig. 4, these results illustrate an important point. Although conclusions drawn from analytical solutions of the rate equations for limiting cases can provide useful insight, one should not assume that such conclusions are generally applicable. Further, even the predictions of somewhat more detailed models that use only static sink distributions may be misleading. Microstructural evolution and the competition for point defects is more dynamic than simple models can easily capture.

2.3. Modifications to model: Incascade interstitial clustering

A second modification of the model involved the addition of incascade interstitial clustering. For simplicity, only di-, tri-, and tetra-interstitial clusters were assumed to form by this mechanism. This is in conflict with the MD cascade simulations in which clusters up to a size of 13 have been observed in iron and up to 15 in copper at elevated temperatures [9–14]; however, it captures the essence of the observed cluster distributions and should be adequate to investigate the importance of the phenomenon. These interstitial clusters are still assumed to be sessile for this initial study.

The implementation of this modification involved reducing the interstitial generation rate by the assumed clustering fraction and adding the appropriate source terms to the rate equations describing the evolution of the small interstitial clusters. If f_{icl}^2, f_{icl}^3, and f_{icl}^4 are the fraction of interstitials found in clusters of size 2, 3, and 4, respectively, and $f_{\mathrm{icl}}^{\mathrm{T}} = (f_{\mathrm{icl}}^2 + f_{\mathrm{icl}}^3 + f_{\mathrm{icl}}^4$; the corrected interstitial generation rate (G_{i}) and the new cluster generation rates (G_{i}^j) are given by the following equations:

$$G_{\mathrm{i}} = G_{\mathrm{dpa}} \cdot \eta \cdot \left(1 - f_{\mathrm{icl}}^{\mathrm{T}}\right) + G_{\mathrm{i-icl}} \tag{1}$$

$$G_{\mathrm{i}}^j = G_{\mathrm{dpa}} \cdot \eta \cdot \frac{f_{\mathrm{icl}}^j}{j}; \quad j = 2, 3, 4 \tag{2}$$

where G_{dpa} is the NRT atomic displacement rate and η is the average cascade survival efficiency, taken here as 0.33. The $G_{\mathrm{i-icl}}$ term in Eq. (2) accounts for the thermal emission of interstitials from di- and tri-interstitial clusters as in Ref. [4].

The need for an internal accounting algorithm to verify conservation of mass in models such as these was mentioned above. An additional check should also be performed to verify that differential point defect partitioning does not occur in the absence of a biased reaction between either type of point defect and any sink. The zero bias calculation is accomplished by setting all the defect capture efficiencies in the model to 1.0, and verifying that no microstructural changes occur, and that $D_{\mathrm{v}}C_{\mathrm{v}} = D_{\mathrm{i}}C_{\mathrm{i}}$ at steady state. This latter equality is actually $D_{\mathrm{v}}(C_{\mathrm{v}} - C_{\mathrm{v}}^{\mathrm{e}}) = D_{\mathrm{i}}C_{\mathrm{i}}$ at temperatures where the thermal equilibrium vacancy concentration, $C_{\mathrm{v}}^{\mathrm{e}}$, is significant. Any deviation from this equality implies that there is some effective bias operating, either due to an error in the model or the oversight of some driving force for no point defect partitioning. For example, a higher-than-equilibrium gas pressure in the small helium bubbles that are a component of the cavity swelling model inhibits vacancy emission from the bubbles. This leads to their absorbing a net vacancy flux with the effect that $D_{\mathrm{v}}C_{\mathrm{v}} < D_{\mathrm{i}}C_{\mathrm{i}}$ in the absence of any other bias. Since one of the effects of incascade interstitial clustering has been referred to as a production bias, the revised model was carefully checked to verify that no spurious bias effect was present.

3. Impact of incascade interstitial clustering

Although a number of cases and parametric variations have been investigated, the results presented here will focus on the temperatures of 350 and 500°C. The former

temperature is in the regime where microstructural transients are more significant and the latter is representative of the high swelling regime in austenitic stainless steel. For ease of interpretation, results will be shown only for the variation of f_{icl}^2. The results obtained for nonzero f_{icl}^3 and f_{icl}^4 are qualitatively similar. No attempt was made to adjust the predictions of the model to fit the data shown above; model parameters other than those specifically mentioned remained as reported previously [4]. The same fast reactor or fusion relevant displacement rate of 10.6 dpa/s was used, but results are presented as a function of irradiation time rather than dose.

Since the formation of interstitial clusters directly within the cascade provides an easy nucleation path, the primary impact of a nonzero f_{icl}^2 was expected to be an increase in the density of faulted dislocation loops. This effect is demonstrated in Fig. 8a and b for the temperatures of 350 and 500°C, respectively. Even the very small value of $f_{icl}^2 = 10^{-5}$ has a dramatic impact on the loop density. Higher values of f_{icl}^2 quickly lead to loop densities and sink strengths that are much higher than is physically reasonable, e.g. loop densities greater than 10^{24} m^{-3}.

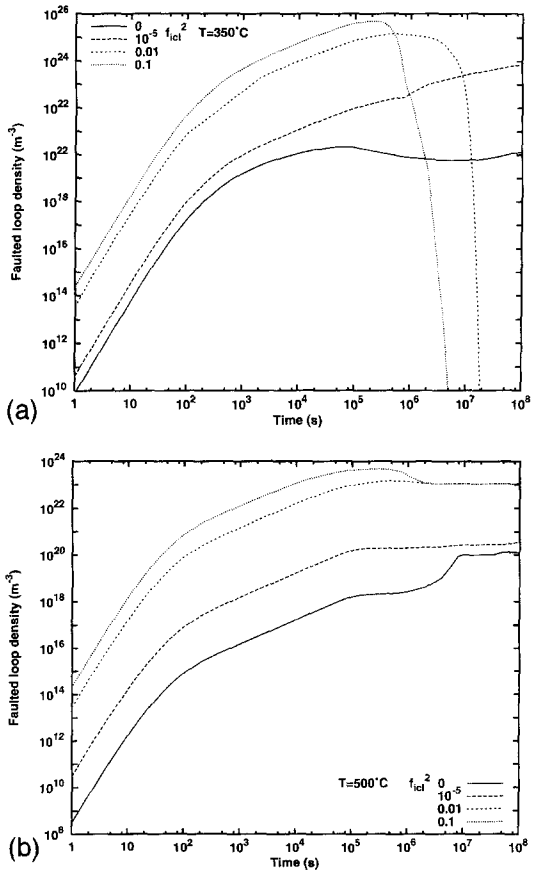

Fig. 8. Influence of the di-interstitial clustering fraction (f_{icl}^2) on the faulted loop number density at 350 (a) and 500°C (b).

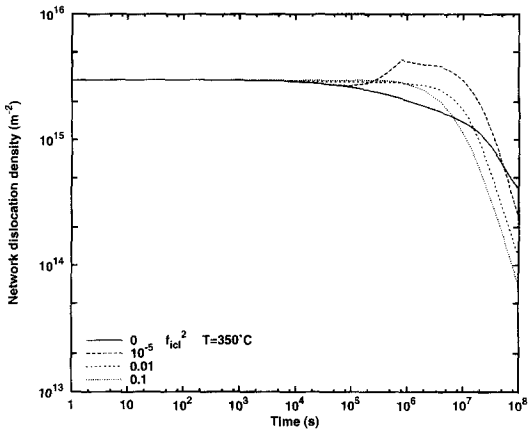

Fig. 9. Influence of the di-interstitial clustering fraction (f_{icl}^2) on the network dislocation density at 350°C.

Indeed, this was one initial criticism of the production bias when it was proposed. In the absence of some mechanism to remove these small loops, they completely dominate the material response. The possibility of easy 1-dimensional loop glide as described by Trinkaus et al. [22] is generally consistent with the interstitial cluster mobilities observed in MD simulations [12–14,19] and provides a plausible solution to this problem. The impact of interstitial cluster mobility is being investigated by a number of researchers; detailed modeling requires the development of a self-consistent set of sink strengths to permit both 1-dimensional and 3-dimensional diffusion in the same model [22,32].

The sharp drop in the loop density for the higher values of f_{icl}^2 at 350°C in Fig. 8a was puzzling, particularly when it was compared with the network dislocation density shown in Fig. 9. The initial increase in the dislocation network for $f_{icl}^2 > 0$ is to be expected since the faulted loops provide a source of line dislocations as they grow and unfault [4,23]. The unexpected loss of the loop source term was accompanied by accelerated recovery of the dislocation network. This behavior can be explained in reference to the somewhat complicated Fig. 10 which plots the ratio $J_R = D_v C_v / D_i C_i$ and the sink strengths as a function of time for $f_{icl}^2 = 0.01$. For reasons that will be discussed below, the values of $J_R/1.25$ and $J_R/1.5$ are also plotted. The time scale of Fig. 10 has been expanded by an additional order of magnitude to show that a second phase of dislocation loop formation occurs beyond 10^8 s.

As mentioned above, if there were no biased interactions in an irradiated material, $D_v C_v$ would equal $D_i C_i$ at steady state and $J_R = 1.0$. Neglecting thermal emission of vacancies, if $J_R < 1.0$ then a neutral sink will receive an excess of interstitials while if $J_R > 1.0$ a neutral sink will receive an excess of vacancies. Extended defects such as vacancy or interstitial clusters can only grow if they receive a net flux of the 'right' type of point defect, while line dislocations can evolve by climb with a net flux of

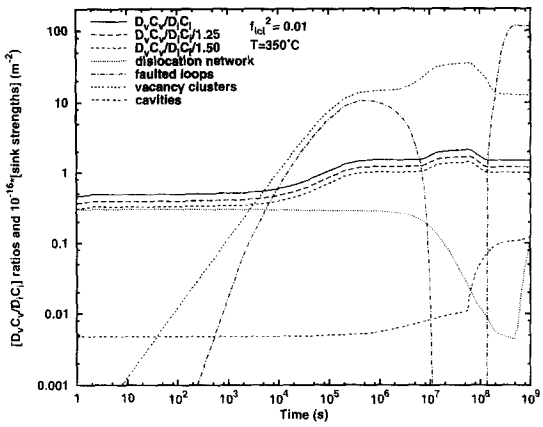

Fig. 10. Time dependent behavior of the point defect flux ratio and sink strengths at 350°C for a di-interstitial clustering fraction (f_{icl}^2) of 0.01. Sink strengths have been multiplied by 10^{-16} to place them on the same scale as the point defect flux ratio.

either type of point defect. A nonsaturable, but essentially neutral sink such as a grain boundary can act as a buffer for the rest of the system.

The conventional system bias attributed to dislocations is a result of dislocations having a greater capture efficiency for interstitials than for vacancies [33]. In the following discussion, the term dislocation bias can be thought of as the ratio of the interstitial to vacancy capture efficiency. A network dislocation/interstitial bias of 25% and a faulted loop/interstitial bias of 50% was used in these calculations [4,23,34]. Thus, the ratios $J_R/1.25$ and $J_R/1.5$ reflect the net flux of either vacancies or interstitials to these biased sinks, depending on whether the appropriate ratio is less than or greater than 1.0. Initially $J_R/1.5 < 1.0$ and the loop nuclei grow by absorbing excess interstitials. At about 4×10^5 s, $J_R/1.5 \approx 1.0$ and a near stationary loop population is obtained. However, J_R continues to increase and the loops are annihilated by an excess vacancy flux. The loop density falls to a very low value in spite of the fact that di-interstitials are being formed continuously within the cascades.

The increase in the vacancy flux at 4×10^5 s arises from the evolution of the incascade vacancy clusters. Until the vacancy cluster population approaches its (temporary) steady state value and vacancy emission from the clusters begins to compensate for the vacancies lost to these clusters within the cascades, the vacancy flux is suppressed. This is essentially equivalent to a vacancy 'production bias' and the vacancy cluster sink strength has been increased by the absence of the interstitials which are tied up in the incascade interstitial clusters. At a slightly earlier time the dislocation network begins to recover by vacancy absorption since $J_R/1.25 > 1.0$. The loss of dislocation and dislocation loop sink strength from the system permits J_R to slightly increase, leading to a further increase in the vacancy cluster population to a new, and still temporary 'steady state.' The excess vacancy flux is able to be maintained because of the incascade interstitial clustering.

Finally, at about 5×10^7 s the cavity sink strength begins to influence the results when void swelling begins as helium-stabilized bubbles convert to voids [4,35,36]. Vacancy absorption by the voids modifies the point defect partitioning and J_R begins to decrease. This leads to a reduction in the vacancy cluster sink strength and dislocation loop growth is once again possible. The increasing loop population leads in turn to an increase in the network dislocation density. Similar results are seen at 500°C but the influence of incascade vacancy clusters is much reduced at the higher temperature. Although details of the time dependence of the point defect concentrations and sink structure shown in Fig. 10 are certainly dependent on the specific parameters used, this discussion serves to illustrate the possible complexity of microstructural evolution. The evolution of all the sinks is coupled by their competition for the available point defects.

Since the influence of incascade interstitial clustering

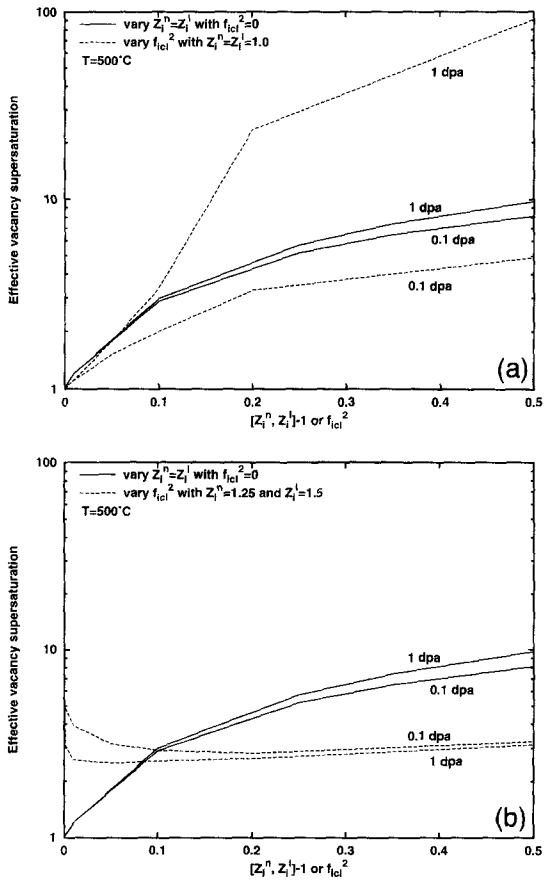

Fig. 11. Dependence of the effective vacancy supersaturation on the dislocation/interstitial bias ($Z_i^n = Z_i^l$) and di-interstitial clustering fraction at doses of 0.1 and 1 dpa. In part (a), the dislocation bias is set to zero in the f_{icl}^2 curves while in (b) $Z_i^n = 1.25$ and $Z_i^l = 1.50$ in the f_{icl}^2 curves.

can also give rise to an effective bias, it is interesting to compare the relative magnitude of this bias with the dislocation/interstitial bias. One way to make such a comparison is to evaluate their individual impact on the effective vacancy supersaturation, S, during irradiation, where:

$$S = \frac{D_v C_v - D_i C_i}{D_v C_v^e} \tag{3}$$

If there is no net system bias, then $S = 1.0$. The critical cavity size for void formation is a strong function of S [4,35,36], so it provides a measure of the swelling susceptibility of a material under a given irradiation condition.

Fig. 11a and b show the effect of both the dislocation bias and the di-interstitial clustering fraction (or production bias) on the effective vacancy supersaturation at 500°C at two doses, 0.1 and 1.0 dpa. The solid curves in both parts of the figure were calculated with a varying network dislocation/interstitial bias (Z_i^n) equal to the faulted loop/interstitial bias (Z_i^l) and the di-interstitial clustering fraction set to zero. In Fig. 11a the dashed curves were calculated for various values f_{icl}^2 and both dislocation/interstitial biases set to zero ($Z_i^n = Z_i^l = 1.0$) while in Fig. 11b the dashed curves reflect variations f_{icl}^2 with the dislocation/interstitial biases set to their nominal values ($Z_i^n = 1.25$ and $Z_i^l = 1.5$).

There is no reason a priori to expect the effect of a given Z_i^n and Z_i^l to correspond to that of any particular value of f_{icl}^2, the range of 0 to 0.5 was chosen since it is consistent with the physically reasonable values for the parameters. Fig. 11a demonstrates that $S = 1.0$ in the absence of any bias; this is a restatement of the requirement mentioned above that $D_v(C_v - C_v^e) = D_i C_i$. The effect of both bias mechanisms is seen to lead to higher values of S. The magnitude of the effect is comparable for either mechanism with the production bias increasing more strongly at the higher dose.

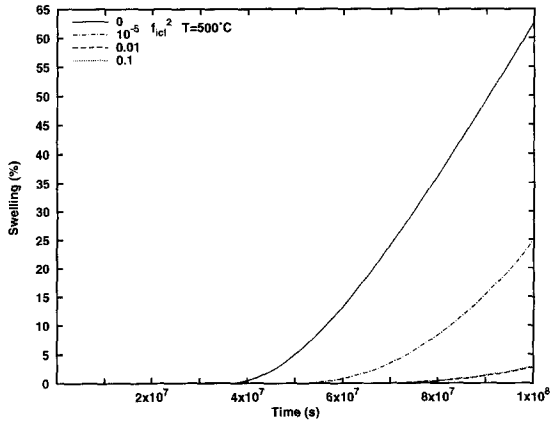

Fig. 12. Influence of the di-interstitial clustering fraction (f_{icl}^2) on the predicted swelling at 500°C, curves for $f_{ilc}^2 = 0.01$ and 0.1 are nearly identical.

A more realistic comparison is shown in Fig. 11b where the effect of incascade clustering is evaluated as an addition to, rather than in lieu of the dislocation/interstitial bias. In this case higher values of f_{icl}^2 actually decrease S until the value of f_{icl}^2 exceeds about 0.25. This is reflected in the calculated swelling values shown in Fig. 12. Increased values f_{icl}^2 or production bias lead to reduced swelling. This arises from the higher total dislocation density which reduces both C_v and C_i, leading to a lower value of S, and a longer swelling incubation time. The experimentally observed swelling is consistent with the value calculated without any incascade interstitial clustering [4].

4. Discussion and summary

A previously developed microstructural model has been modified to reflect recent insights on primary defect formation obtained from molecular dynamics cascade simulations and to explore the impact of the commonly used approximation of steady state point defect concentrations. Elimination of the steady state assumption has been shown to somewhat improve the agreement between the predictions of the model and low temperature irradiation data. The model was also used to demonstrate the importance of microstructural transients as they influence the point defect concentrations. By tracking the fate of the radiation-induced point defects, the relative importance of the different microstructural sinks was shown to be a function of both irradiation temperature and dose. The overall result of these observations is to suggest that the simple, limiting cases which permit analytical solutions for the rate equations may rarely occur in practice. An interpretation of experimental results which is based on such simple models may be suspect.

The potentially significant role of incascade interstitial clustering has been highlighted by the complex time-dependence of the point defect concentrations and sink structure. In the absence of a mechanism to remove these clusters, the microstructure would be rapidly dominated by interstitial loops. Weidersich has investigated incascade clustering using a different mathematical approach than that followed here [37]. His results also highlighted the important effect that these clusters can have on the point defect concentrations. Although it is expected that some of the effects discussed above would be minimized by permitting the interstitial clusters and small loops to glide to sinks, the primary conclusion should hold. That is, microstructural evolution is a complex phenomenon, with the point defect concentrations providing the coupling for the various sinks to influence one another.

Finally, a limited comparison of the conventional dislocation bias and a primitive version of the so-called production bias on a common basis suggests that the importance

of the latter may have been overestimated in the case of engineering alloys. When a reasonable value of the dislocation/interstitial bias was included in the analysis, the addition of incascade clustering tended to reduce the predicted swelling at 500°C to values well below that observed experimentally. It is not simple to predict what the additional effect would be if the interstitial clusters were glissile as in the current version of the production bias. Mobility would reduce the sink strength contribution from the clusters and, considering only this factor, should increase S and reduce the swelling incubation time for $f_{\mathrm{icl}}^2 > 0$ in Fig. 12. However, the effect will depend on the details of how the mobile clusters move and interact with the other sinks and each other. Different behavior should be expected for simple 1-dimensional diffusion, 1-dimensional diffusion with trapping and a change of the glide plane, or 3-dimensional diffusion [22]. Similarly, an elastic interaction could lead to preferential absorption of the clusters by dislocations or trapping could reduce the effective cluster mobility.

There is some conflict between the success of the kinetic models that have not included incascade interstitial clustering and the high interstitial clustering fractions that are predicted by the MD cascade simulations. These kinetic models have been able to successfully fit a broad range of data from irradiation experiments. Since the MD results suggest that relevant physics is being neglected, the models must be accounting for this in some other manner. For example, an effective interstitial migration energy of 0.85 eV was required in Ref. [4] to obtain agreement between the faulted loop density data and the model predictions. This high value was initially attributed to trapping [4], but it may have been acting as a surrogate for incascade interstitial clustering. Another explanation is the mobility of the interstitial clusters. As stated above, if these clusters are produced to any significant degree, they must be mobile to prevent a physically unreasonable sink strength from developing. However, even if the MD simulations adequately represent cluster mobility in pure metals, it is reasonable to suspect that trapping by impurities or solutes could reduce their mobility in alloys. Further, their preferential loss to sinks other than cavities may be required to obtain reasonable swelling rates. In this case, their impact becomes more analogous to the conventional dislocation/interstitial bias and may be accounted for by an 'effective' bias which either over or underestimates the actual elastic interaction.

Because the evidence of the MD simulations is so compelling, additional work with the present model is planned in order to include mobile interstitial clusters to obtain a more complete evaluation of the production bias. Similar work is underway with the ferritic steel embrittlement model described in Refs. [6,7,38]. However, it is worth noting that an effective system bias can arise in many ways. For example, a model developed to investigate radiation damage in ceramic oxides demonstrated that a bias existed (i.e. $S > 0$) if one of the point defect properties such as the vacancy migration energy had different values on the two sublattices [39]. This bias was present even if there were no differences in sink capture efficiencies. Void swelling, like other types of microstructural evolution, requires the net partitioning of vacancies and interstitials between the various extended defects; whether they arrive singly or in clusters may be less significant. It is not primarily the way in which primary damage occurs, but the way in which the point defects are absorbed which gives rise to microstructural evolution. In this sense, the dislocation/interstitial bias, the production bias, and other possible mechanisms can all be thought of as contributing to a point defect survival bias.

References

[1] A.D. Brailsford and R. Bullough, Philos. Trans. R. Soc. London 302 (1981) 87–137.

[2] L.K. Mansur, Nucl. Technol. 40 (1978) 5–34.

[3] P.T. Heald, Philos. Mag. 31 (1975) 551–558.

[4] R.E. Stoller and G.R. Odette, in: Radiation-Induced Changes in Microstructure, ASTM STP 955, eds. E.A. Garner, N.H. Packan and A.S. Kumar (American Society of Testing and Materials, Philadelphia, 1987) pp. 371–392.

[5] R.E. Stoller, M.L. Grossbeck and L.K. Mansur, in: Effects of Radiation on Materials, ASTM STP 1125, eds. R.E. Stoller, A.S. Kumar and D.S. Gelles (American Society of Testing and Materials, Philadelphia, 1992) pp. 517–529.

[6] R.E. Stoller, in: Effects of Radiation on Materials, ASTM STP 1270 (American Society of Testing and Materials, Philadelphia, 1996) pp. 25–59.

[7] R.E. Stoller, in: Effects of Radiation on Materials, ASTM STP 1175, eds. A.S. Kumar, D.S. Gelles, R.K. Nanstad and E.A. Little (American Society of Testing and Materials, Philadelphia, 1993) pp. 394–426.

[8] R.E. Stoller and L.K. Mansur, Radiation Materials Science, Proc. of Int. Conf., Vol. 1, Kharkov, Ukraine, 1990, pp. 52–67.

[9] T. Diaz de la Rubia and W.J. Phythian, J. Nucl. Mater. 191–194 (1992) 108–115.

[10] A.J.E. Foreman, C.A. English and W.J. Phythian., Philos. Mag. A 66 (1992) 655–669; A.J.E. Foreman, W.J. Phythian and C.A. English, Philos. Mag. A 66 (1992) 671–695.

[11] A.F. Calder and D.J. Bacon, J. Nucl. Mater. 207 (1993) 25–45.

[12] W.J. Phythian, R.E. Stoller, A.J.E. Foreman, A.F. Calder, and D.J. Bacon, J. Nucl. Mater. 223 (1995) 245–261.

[13] R.E. Stoller, in: Microstructure of Irradiated Materials, eds. I.M. Robertson, L.E. Rehn, S.J. Zinkle and W.J. Phythian (Materials Research Society, Pittsburgh, PA, 1995) pp. 21–26.

[14] R.E. Stoller, Point Defect Survival and Clustering Fractions Obtained from Molecular Dynamics Simulations of High Energy Cascades, presented at the Seventh Int. Conf. on Fusion Reactor Materials, Obninsk, Russia, September 25–29, 1995, to be published in J. Nucl. Mater.

[15] D.J. Bacon and T. Diaz de la Rubia, J. Nucl. Mater. 216 (1994) 275–290.
[16] D.J. Bacon, A.F. Calder, F. Gao, V.G. Kapinos, and S.J. Wooding, Nucl. Instrum. Methods in Phys. Res. B 102 (1995) 37–46.
[17] M.J. Norgett, M.T. Robinson and I.M. Torrens, Nucl. Eng. Des. 33 (1975) 50.
[18] R.E. Stoller, J. Nucl. Mater., to be submitted.
[19] B.D. Wirth, G.R. Odette, D. Maroudas and G.E. Lucas, these Proceedings, p. 185.
[20] C.H. Woo and B.N. Singh, Phys. Status Solidi (b) 159 (1990) 609–616.
[21] C.H. Woo and B.N. Singh, Philos. Mag. A 65 (1992) 889–912.
[22] H. Trinkhaus, B.N. Singh and A.J.E. Foreman, J. Nucl. Mater. 206 (1993) 200–211.
[23] R.E. Stoller, Microstructural Evolution in Fast-Neutron-Irradiated Austenitic Stainless Steels, ORNL-6430 (Oak Ridge National Laboratory, Oak Ridge, TN, 1987).
[24] F.A. Garner, in: Optimizing Materials for Nuclear Applications (AIME, New York, 1984) pp. 111–139.
[25] P.J. Maziasz, in: Alloy Development for Irradiation Performance: Semiannual Progress Report, DOE/ER-0045/7 (U.S. DOE Office of Fusion Energy, Washington, March 1982) pp. 54–97.
[26] J.I. Bramman, C. Brown, J.S. Watkin, C. Cawthorne, E.J. Fulton, P.J. Barton and E.A. Little, Radiation Effects in Breeder Reactor Structural Materials (AIME, New York, 1977) pp. 479–507.
[27] H.R. Brager and J.L. Straalsund, J. Nucl. Mater. 46 (1973) 134–158.
[28] P.J. Barton, B.L. Eyre and D.A. Stow, J. Nucl. Mater. 67 (1977) 181–197.
[29] H.R. Brager, J. Nucl. Mater. 57 (1975) 103–118.
[30] H.R. Brager, F.A. Garner and G.L. Guthrie, J. Nucl. Mater. 66 (1977) 181–197.
[31] E.E. Bloom and J.O. Stiegler, in: Effect of Radiation on Substructure and Mechanical Properties of Metals and Alloys, ASTM STP 529 (ASTM, Philadelphia, 1973) pp. 360–382.
[32] U. Gösele and A. Seeger, Philos. Mag. 34 (1976) 177–193.
[33] L.K. Mansur, A.D. Brailsford and W.G. Wolfer, J. Nucl. Mater. 105 (1982) 36–38.
[34] W.G. Wolfer, in: Fundamental Aspects of Radiation Damage in Metals, CONF-751006-P2 (U.S. National Technical Information Service, Springfield, VA, 1975) pp. 812–819.
[35] R.E. Stoller and G.R. Odette, J. Nucl. Mater. 131 (1983) 118–125.
[36] R.E. Stoller and G.R. Odette, in: Radiation-Induced Changes in Microstructure, ASTM STP 955, eds. E.A. Garner, N.H. Packan and A.S. Kumar (American Society of Testing and Materials, Philadelphia, 1987) pp. 358–371.
[37] H. Weidersich, in: Physics of Irradiation Effects in Metals PM'91, ed. G. Szenes Materials Science Forum 97–99 (Trans. Tech. Publications, Zurich, 1992) pp. 59–73.
[38] R.E. Stoller, The Impact of Mobile Point Defect Clusters in a Kinetic Model of Pressure Vessel Embrittlement, presented at the 18th Int. Symp. on the Effects of Radiation on Materials, Hyannis, MA, USA, 25–27 June, 1996, Am. Soc. Testing Mater., to be submitted.
[39] R.E. Stoller, J. Am. Cer. Soc. 73 (1990) 2446–2451.